Article

Towards Zirconium Phosphonate-Based Microarrays for Probing DNA#Protein Interactions: Critical Influence of the Location of the Probe Anchoring Groups

Julien Monot, Marc Petit, Sarah M. Lane, Isabelle Guisle, Jean Léger, Charles Tellier, Daniel R. Talham, and Bruno Bujoli

J. Am. Chem. Soc., **2008**, 130 (19), 6243-6251 • DOI: 10.1021/ja711427q • Publication Date (Web): 12 April 2008

J|A|C|S
ARTICLES

Published on Web 04/12/2008

Towards Zirconium Phosphonate-Based Microarrays for Probing DNA−Protein Interactions: Critical Influence of the Location of the Probe Anchoring Groups

Julien Monot,[†] Marc Petit,[†] Sarah M. Lane,[‡] Isabelle Guisle,[§] Jean Léger,[§] Charles Tellier,[||] Daniel R. Talham,*[,‡] and Bruno Bujoli*[,†]

Université de Nantes, CNRS, UMR 6230, Chimie Et Interdisciplinarité: Synthèse Analyse Modélisation (CEISAM), UFR Sciences et Techniques, 2, rue de la Houssinière, BP 92208, 44322 NANTES Cedex 3, Department of Chemistry, University of Florida, Gainesville, Florida, 32611-7200, USA, U INSERM 533, UFR de Médecine Physiologie, 1 rue Gaston Veil, BP 53508, 44035 NANTES Cedex 1, France, and Nantes Atlantique Universités, CNRS, UMR 6204, Laboratoire de Biotechnologie, Biocatalyse et Biorégulation, 2 Rue de la Houssinière, BP92208, 44322 Nantes Cedex 03, France

Received December 27, 2007; E-mail: Bruno.Bujoli@univ-nantes.fr; talham@chem.ufl.edu

Abstract: Terminal phosphate groups on double-stranded DNA probes bind strongly to glass substrates coated with a zirconium phosphonate monolayer, and probes immobilized in this way as microarrays can be used to detect protein targets. The sensitivity of the microarray was shown to be enhanced by the use of a polyguanine segment ($(G)_n$, $n \geq 5$) as a spacer between the phosphate linker and the protein interaction domain. More importantly, the presence of phosphate linkers on both ends of the dsDNA probes leads to significant enhancement of target capture. The relevant characteristics of the different probes when bound to the surface were determined, by the original use of a combination of surface characterization techniques (XPS, AFM, and Sarfus). In this context, the location of the phosphate linkers in the duplex probes was found to result in different probe surface coverage and presentation on the surface, which affect subsequent interactions with the target protein.

Introduction

DNA arrays have emerged as a convenient tool in molecular biological research, used for rapid and accurate gene mapping, DNA sequencing, mRNA expression analysis, and diagnosis of genetic diseases.[1–4] Typical strategies consist of single-stranded oligonucleotides of different sequences, called probes, bound to a surface and amenable to subsequent hybridization by targets. Recently, these in vitro microarray technologies have been extended to double-stranded DNA (dsDNA) arrays for high-throughput characterization of DNA–protein interactions. Indeed, solid-surface coupled dsDNA has showed great potential for the highly parallel analysis of DNA-binding proteins such as transcription factors,[5] predicting DNA binding sites,[6,7] assessing binding affinity,[8,9] and screening sequence specific DNA-binding drugs.[10] Therefore, the fabrication of fast, economical, and informative dsDNA-coupled solid entities becomes a pivotal problem for extensive application of surface coupled dsDNA.

At this time, there are relatively few options for the immobilization of dsDNAs to slide surfaces. Generally, unmodified dsDNA obtained by PCR (60–1500 bp long) can be attached randomly by UV cross-linking,[2] for example, on polylysine slides. These methods suffer drawbacks as the DNA structure can be perturbed by multiple cross-links to the slide surface, or in the absence of the cross-links, a significant percentage of the DNA molecules will not be attached to the slides. Alternatively, single-stranded DNA (ssDNA) can be end-attached, either by a reactive group at one of the DNA termini or by *in situ* synthesis of arrays of oligonucleotides,[11] and then subsequently made double-stranded by hybridization.[7] These methods suffer from two main problems. One is the high costs of the synthesis of the complementary ssDNA oligonucleotides and their amino modification. The other more important problem is that the method cannot fabricate dsDNA microarrays carrying

[†] Chimie Et Interdisciplinarité: Synthèse Analyse Modélisation.
[‡] University of Florida.
[§] UFR de Médecine Physiologie.
[||] Laboratoire de Biotechnologie, Biocatalyse et Biorégulation.

(1) *Nat. Genet.* **1999**, *21*, 1–60.
(2) DeRisi, J.; Penland, L.; Brown, P. O.; Bittner, M. L.; Meltzer, P. S.; Ray, M.; Chen, Y.; Su, Y. A.; Trent, J. M. *Nat. Genet.* **1996**, *14* (4), 457–60.
(3) Shoemaker, D. D. *Nature* **2001**, *409* (6822), 922 ff.
(4) Wang, J. *Nucleic Acids Res.* **2000**, *28* (16), 3011–3016.
(5) Mukherjee, S.; Berger, M. F.; Jona, G.; Wang, X. S.; Muzzey, D.; Snyder, M.; Young, R. A.; Bulyk, M. L. *Nat. Genet.* **2004**, *36* (12), 1331–9.
(6) Bulyk, M. L.; Huang, X.; Choo, Y.; Church, G. M. *Proc. Natl. Acad. Sci. U.S.A.* **2001**, *98* (13), 7158–63.
(7) Krylov, A. S.; Zasedateleva, O. A.; Prokopenko, D. V.; Rouviere-Yaniv, J.; Mirzabekov, A. D. *Nucleic Acids Res.* **2001**, *29* (12), 2654–60.
(8) Doi, N.; Takashima, H.; Kinjo, M.; Sakata, K.; Kawahashi, Y.; Oishi, Y.; Oyama, R.; Miyamoto-Sato, E.; Sawasaki, T.; Endo, Y.; Yanagawa, H. *Genome Res.* **2002**, *12* (3), 487–92.
(9) Shumaker-Parry, J. S.; Aebersold, R.; Campbell, C. T. *Anal. Chem.* **2004**, *76* (7), 2071–82.
(10) Drobyshev, A. L.; Zasedatelev, A. S.; Yershov, G. M.; Mirzabekov, A. D. *Nucleic Acids Res.* **1999**, *27* (20), 4100–5.
(11) Hughes, T. R.; et al. *Nat Biotechnol* **2001**, *19* (4), 342–7.

sequence-similar probes, such as probes with single nucleotide variation. Some solutions to this problem have been found with in situ synthesized dsDNA from ssDNA either by primer extension[6,12] or by self-hairpairing.[13,14] Typically, the ssDNA sequence has a constant priming sequence at the 3′-end that allows a common primer to be annealed and used for on-chip primer extension reactions that produced dsDNA molecules.[15] In the second method, immobilized ssDNA containing two reverse complementary sequences at the 3′ hydroxyl end are annealed to form a short dsDNA hairpin structure that provides the primer for later polymerase reaction. However, there are still advantages to directly spotting dsDNA molecules since they can be created in a quality-controlled manner in solution. Also, direct spotting can be used with long dsDNA probe sequences accessible by PCR.

The ssDNA arrays rely on covalent attachment of the DNA through reactive function introduced at the end, usually the 5′-end, of the oligonucleotide probe. Several combinations of surface/oligonucleotide function have been demonstrated including thiol/acrylamide,[16] activated carboxylic acid/amine,[17,18] amine/aldehyde,[19–21] epoxide/amine,[22] and biotin/streptavidin.[23–25] With these specific linkages, the population of probes is attached in a homogeneous manner with good surface coverage but requires specific chemical modification of the oligonucleotides, which are not naturally present in DNA molecules.

We recently reported a fundamentally different route for covalently attaching oligonucleotide probes to surfaces for array applications that use metal/ligand interactions to selectively immobilize the probes. In contrast to organic covalent linkages, the use of "organic−inorganic" interactions to immobilize oligonucleotide probes into arrays on a surface has largely remained unexplored. The principal exception is the use of thiol-derivatized oligonucleotides to attach to metallic gold via a sulfur−gold linkage, although use in array applications is limited.[26–29] In our approach, slides are modified with a zirconium-phosphonate surface layer that is known to strongly immobilize phosphate or phosphonate functionalized molecules[30–35] through a coordinate covalent interaction between the terminal $ROPO_3^{2-}$ or RPO_3^{2-} groups and the inorganic ions on the surface. Taking advantage of this chemistry, phosphate terminated oligonucleotides were found to selectively bind to this mixed organic/inorganic monolayer although nonphosphorylated oligonucleotides did not, and the methodology was used to form efficient oligonucleotide arrays (see Supporting Information).[36] Recently, phosphorylated oligonucleotides were also shown to covalently bind to epoxide-functionalized glass surfaces.[37]

In this paper, we show that the metal/ligand approach to immobilizing oligonucleotide probes can be extended to dsDNA probes. Terminal phosphate groups on double-stranded probes bind strongly to glass substrates coated with a zirconium phosphonate monolayer, and probes immobilized in this way can be used to detect protein targets. Several features of the probes are shown to influence the efficacy of protein capture. Among these are the use of a spacer between the phosphate linker and the protein interaction domain. Earlier work on ssDNA probes revealed that the use of a polyguanine segment as a spacer between the probe sequence and surface linkage led to enhanced target oligonucleotide capture.[36] A similar influence is shown here for dsDNA probes. The efficacy of binding probes to the surface through the terminal phosphate groups according to their location is explored with extensive surface chemical analysis, and the sensitivity and specificity of the arrays for detecting protein targets are evaluated using a dsDNA/protein interaction model.[38] The number and location of the phosphate linker in the duplex probes were also varied, including examples with linkers on both ends of the dsDNA probes. Importantly, the use of linkers on both ends of the dsDNA probe is shown to have a significant influence on the extent of target capture.

Experimental Section

Materials. Glass substrates were purchased from Gold Seal Products (cat no. 3010, 3 × 1″, thickness 0.93 to 1.05 mm). Oligonucleotides were purchased from SIGMA GENOSYS with the following structures (C = cytosine, G = guanine, A = adenine, *T* = thymine): 5′-$(H_2O_3PO)_x$-$(G)_n$-AATCCTCG[*AAAATTATTAAATATACAT*]TTGATTTTAT-$(G)_p$-$(OPO_3H_2)_y$-3′, **5′P-X** ($x = 1$ and $n = p = y = 0$), **5′P-(G)$_n$-X** ($x = 1$, $n = 1, 3, 5, 7, 8, 9$, $p = y = 0$), **X-(G)$_9$-P3′** ($y = 1$, $p = 9$, $x = n = 0$), **5′P-(G)$_9$-X-(G)$_9$-P3′** ($x = y = 1$, $n = p = 9$); 5′-(H_2O_3PO)-(ATCGGCGAG)-AATCCTC-

(12) Bulyk, M. L.; Gentalen, E.; Lockhart, D. J.; Church, G. M. *Nat. Biotechnol.* **1999**, *17* (6), 573–7.
(13) Wang, J.; Bai, Y.; Li, T.; Lu, Z. *J. Biochem. Biophys. Methods* **2003**, *55* (3), 215–32.
(14) Warren, C. L.; Kratochvil, N. C.; Hauschild, K. E.; Foister, S.; Brezinski, M. L.; Dervan, P. B.; Phillips, G. N., Jr.; Ansari, A. Z. *Proc. Natl. Acad. Sci. U.S.A.* **2006**, *103* (4), 867–72.
(15) Berger, M. F.; Philippakis, A. A.; Qureshi, A. M.; He, F. S.; Estep, P. W.; Bulyk, M. L *Nat. Biotechnol.* **2006**, *24* (11), 1429–35.
(16) Mielewczyk, S.; Patterson, B. C.; Abrams, E. S.; Zhang, T. Patent WO0116372, 2001.
(17) Beier, M.; Hoheisel, J. D. *Nucleic Acids Res.* **1999**, *27* (9), 1970–1977.
(18) Demers, L. M.; Park, S. J.; Taton, T. A.; Li, Z.; Mirkin, C. A. *Angew. Chem., Int. Ed.* **2001**, *40* (16), 3071–3073.
(19) Guschin, D.; Yershov, G.; Zaslavsky, A.; Gemmell, A.; Shick, V.; Proudnikov, D.; Arenkov, P.; Mirzabekov, A. *Anal. Biochem.* **1997**, *250* (2), 203–211.
(20) MacBeath, G.; Schreiber, S. L. *Science* **2000**, *289* (5485), 1760–1763.
(21) Melnyk, O.; Olivier, C.; Ollivier, N.; Hot, D.; Hout, L.; Lemoine, Y.; Wolowczuk, I.; Huynh-Dinh, T.; Gouyette, C.; Gras-Masse, H. Patent WO0142495, 2001.
(22) Osborne, M. A.; Barnes, C. L.; Balasubramanian, S.; Klenerman, D. *J. Phys. Chem. B* **2001**, *105* (15), 3120–3126.
(23) Gilles, P. N.; Wu, D. J.; Foster, C. B.; Dillon, P. J.; Chanock, S. J. *Nat. Biotechnol.* **1999**, *17* (4), 365–370.
(24) Wennmalm, S.; Edman, L.; Rigler, R. *Chem. Phys.* **1999**, *247* (1), 61–67.
(25) Wennmalm, S.; Rigler, R. *J. Phys. Chem. B* **1999**, *103* (13), 2516–2519.
(26) Brockman, J. M.; Frutos, A. G.; Corn, R. M. *J. Am. Chem. Soc.* **1999**, *121* (35), 8044–8051.
(27) Georgiadis, R.; Peterlinz, K. P.; Peterson, A. W. *J. Am. Chem. Soc.* **2000**, *122* (13), 3166–3173.
(28) Herne, T. M.; Tarlov, M. J. *J. Am. Chem. Soc.* **1997**, *119* (38), 8916–8920.
(29) Levicky, R.; Herne, T. M.; Tarlov, M. J.; Satija, S. K. *J. Am. Chem. Soc.* **1998**, *120* (38), 9787–9792.
(30) Benitez, I. O.; Bujoli, B.; Camus, L. J.; Lee, C. M.; Odobel, F.; Talham, D. R. *J. Am. Chem. Soc.* **2002**, *124* (16), 4363–4370.
(31) Byrd, H.; Pike, J. K.; Talham, D. R. *Chem. Mater.* **1993**, *5* (5), 709–715.
(32) Byrd, H.; Whipps, S.; Pike, J. K.; Ma, J. F.; Nagler, S. E.; Talham, D. R. *J. Am. Chem. Soc.* **1994**, *116* (1), 295–301.
(33) Nixon, C. N.; Le Claire, K.; Odobel, F.; Bujoli, B.; Talham, D. R. *Chem. Mater.* **1999**, *11* (4), 965–976.
(34) Petruska, M. A.; Fanucci, G. E.; Talham, D. R. *Chem. Mater.* **1998**, *10* (1), 177–189.
(35) Wu, A. P.; Talham, D. R. *Langmuir* **2000**, *16* (19), 7449–7456.
(36) Nonglaton, G.; Benitez, I. O.; Guisle, I.; Pipelier, M.; Leger, J.; Dubreuil, D.; Tellier, C.; Talham, D. R.; Bujoli, B. *J. Am. Chem. Soc.* **2004**, *126* (5), 1497–1502.
(37) Mahajan, S.; Kumar, P.; Gupta, K. C. *Bioconjugate Chem.* **2006**, *17* (5), 1184–1189.
(38) Snapyan, M.; Lecocq, M.; Guevel, L.; Arnaud, M. C.; Ghochikyan, A.; Sakanyan, V. *Proteomics* **2003**, *3* (5), 647–657.

G[*AAAATTATTAAATATACAT*]TTGATTTTAT termed as **5′P-(Random)-X**; 5′-$(H_2O_3PO)_x$-$(G)_n$-ATAAAATCAA[*ATGTATATT-TAATAATTTT*]CGAGGATT-$(G)_p$-$(OPO_3H_2)_y$-3′, **compX** ($x = n = p = y = 0$), **5′P-compX** ($x = 1$ and $n = p = y = 0$), **5′P-$(G)_n$-compX** ($x = 1$, $n = 1, 3, 5, 7, 8, 9$, $p = y = 0$), **compX-$(G)_9$-P3′** ($y = 1$, $p = 9$, $x = n = 0$); 5′-(H_2O_3PO)-(AGTCGAGGA)-ATAAAATCAA[*ATGTATATTTAATAATTTT*]CGAGGATT termed as **5′P-(Random)-compX**; 5′-(H_2O_3PO)-$(G)_9$-AGGGGCAAGAG-GAGGATCGGCGAGGATGGTAGGATAT termed as **5′P-$(G)_9$-Y;** 5′-(H_2O_3PO)-$(G)_9$-ATATCCTACCATCCTCGCCGATCCTC-CTCTTGCCCCT termed as **5′P-$(G)_9$-compY**. The sequence given in square brackets corresponds to the area of interaction with protein ArgR in the **X/compX** double strand, while the **Y/compY** double strand has no interaction domain with the protein. Reagents were of analytical grade and used as received from commercial sources, unless indicated. Zirconated octadecyl phosphonic acid (ODPA-Zr) modified slides were prepared as described previously.[30]

Protein Expression and Purification. ArgR repressor from *Thermotoga neapolitana* was overexpressed in recombinant *E. coli* BL21 strains carrying the corresponding plasmids.

The culture was grown in Luria-Bertoni medium containing ampicillin (50 μg/mL) at 37 °C until an OD_{600} of 0.6–0.8. After induction using isopropyl-1-β-D-thio-1-galactopyranoside (IPTG) (1 mM), incubation was continued for 5 h. The protein was purified on nickel-nitrilotriacetic acid (Ni-NTA) columns according to the manufacturer's recommendations (Qiagen, Courtaboeuf, France), eluting with a buffer containing NaH_2PO_4 (50 mM, pH 8), NaCl (300 mM), and imidazole (250 mM). The protein concentration was measured using an Agilent 2100 bioanalyzer (Agilent).

Preparation of the dsDNA Probes. The desired ssDNA oligonucleotide (20 μM in 2X SSC [saline sodium citrate, adjusted to pH 6 by addition of HCl]) was mixed with its complementary sequence (20 μM in 2X SSC, pH 6). The mixture was then denatured at 98 °C for 2 min and subsequently hybridized at 60 °C for the **X/compX** sequences or at 74 °C for the **Y/compY** sequences. Finally, the hybridization was fixed at 4 °C for 4 min.

Typical Spotting/Incubation Conditions. The slides were spotted with a quill type pin microarrayer (SDDC2, Virtek) at a 250 μm spacing, using three steel tips and 10 μM dsDNA solutions in 1X SSC. The spotted slides were placed overnight in a sealed slide box at room temperature. To passivate unspotted areas, slides were treated after spotting with a solution of 0.3% α-casein (SIGMA), 3.5X SSC, 0.3% SDS (sodium dodecyl sulfate) at 20 °C for 45 min and then rinsed using a TBS (Tris buffered saline) solution of TrisHCl (20 mM), NaCl (50 mM), and KCl (50 mM) at pH 8 for 5 min.

Incubations were performed by applying an ArgR solution to the microarrays (1 μM in TBS-0.3% α-Casein) for 1 h at 20 °C. Microarrays were washed 3 times with TBS-0.05% Tween 20 for 5 min, and a monoclonal antipolyhistidine antibody (produced in mouse - SIGMA) solution (0.5 μL/mL in TBS-0.3% α-casein) was applied to the microarrays for 1 h at 20 °C. The slides were washed again 3 times with TBS-0.05% Tween 20 for 5 min and incubated with a FluoProbes 642 Goat Anti-Mouse IgG (Interchim) solution (1 μL/mL in TBS-0.3% α-casein) for 1 h at 20 °C. Finally, microarrays were washed 3 times with TBS-0.05% Tween 20 for 5 min and once with ultrapure water and were spun dry centrifuging at 1500 rpm for 1 min. All washes and incubations were performed in small staining jars at 20 °C on an oscillating shaker.

Microarray Analysis. All microarrays were scanned on an HT express ScanArray apparatus (Perkin-Elmer, Wellesley, MA) at two different laser powers to best capture the broad range of signal intensities and avoid saturation of spot intensities. A suitable laser excitation wavelength and emission filter were used to detect Alexa642: 642 nm (excitation), 660 nm (emission). The fluorescence intensities in color images of the slides are color-coded, varying from blue (low) to green, yellow, red, and then white (saturation). The location of each analyte spot on the array was outlined using the mapping software GenePix (Axon Laboratories, Palo Alto, CA). The background, calculated as the median of pixel intensities from the local area around each spot, was subtracted from the average pixel intensity within each spot.

XPS Measurements. The dsDNA spotting solutions (20 μM) were prepared in a 1X SSC buffer (pH 6). To create a spot large enough for XPS analysis, 30 μL of the dsDNA were pipetted onto the rinsed and dried zirconium phosphonate surface. Once the DNA had been spotted, the slides were placed overnight in Petri dishes at room temperature. Then the slides were submerged for 45 min in 3.5X SSC, 0.3% SDS at 20 °C, followed by rinsing five times with nanopure water and spin drying. XPS was performed using a UHV XPS/ESCA PHI 5100 system. Survey scans and multiplex scans (Zr 3d, P 2p, and N 1s) were taken with a Mg Kα X-ray source using a power setting of 300 W and a takeoff angle of 45° with respect to the surface. Survey scans were taken for all samples with a pass energy of 89.4 eV, and multiplex scans were taken with a pass energy of 22.36 eV. Using commercial XPS analysis software and Shirley background subtraction, the peak areas were determined. For each sample, at least four different spots were analyzed.

Sarfus Measurements. Nanometer scale optical images were obtained from a Sarfus 3D apparatus (Nanolane, Montfort-le-Gesnois, France). For optical studies, this equipment included an upright optical microscope (DM4000, Leica Microsystems, Wetzlar, Germany) and specific contrast-enhanced substrates termed Surfs. For optical thickness measurements which is based on color/thickness correspondence, a calibration standard made of nanometric steps and an image treatment software (Sarfusoft 2.0) were used.

The standard Surfs (toplayer SiO_2) were first modified with a zirconated octadecyl phosphonic acid (ODPA-Zr) layer as reported previously.[30] The surfs were then spotted and incubated under conditions similar to those described for the glass slide analogues.

AFM Measurements. The AFM measurements were made in AAC mode (vibrating mode) to prevent any damage to the surface, using a Sarfus/AFM integrated apparatus codeveloped by Scientec (Les Ulis, France) and Nanolane (Montfort-le-Gesnois, France) [See Supporting Information]. Combining AFM (5500LS, Agilent Technologies, USA) with Sarfus allowed rapid and precise optical localization of dsDNA spots under the AFM tip.

CD measurements. The CD spectra of dsDNAs samples (10 μM) prepared in water or in 1X SSC (pH6) were recorded in the 220–320 nm region using a J-810 JASCO (Tokyo, Japan) spectropolarimeter. Samples were loaded in 150 μL quartz cells with a 0.2 cm path length. Three consecutively measured scans taken in a step-by-step mode (0.1 nm) were averaged for the final CD spectra. The ellipticity values are given in millidegrees (mdeg).

Results and Discussion

Zirconium Phosphonate Surface and Spotting Conditions. Zirconium phosphonate modified surfaces are generated by adsorbing Zr^{4+} ions to surface phosphonate or phosphate groups. An active metal layer results when the phosphorylated groups are closely organized into a monolayer so that the Zr^{4+} ions bind to the surface groups to form a layer while retaining some free coordination sites. The starting phosphorylated surfaces can be prepared in different ways, including covalent attachment of the phosphorylated groups to silica[39–47] or gold,[41,42,45,48] and

(39) Horne, J. C.; Blanchard, G. J. *J. Am. Chem. Soc.* **1996**, *118* (50), 12788–12795.
(40) Horne, J. C.; Huang, Y.; Liu, G. Y.; Blanchard, G. J. *J. Am. Chem. Soc.* **1999**, *121* (18), 4419–4426.
(41) Katz, H. E.; Schilling, M. L.; Chidsey, C. E. D.; Putvinski, T. M.; Hutton, R. S. *Chem. Mater.* **1991**, *3* (4), 699–703.
(42) Lee, H.; Kepley, L. J.; Hong, H. G.; Akhter, S.; Mallouk, T. E. *J. Phys. Chem.* **1988**, *92* (9), 2597–2601.
(43) Lee, H.; Kepley, L. J.; Hong, H. G.; Mallouk, T. E. *J. Am. Chem. Soc.* **1988**, *110* (2), 618–620.
(44) Neff, G. A.; Helfrich, M. R.; Clifton, M. C.; Page, C. J. *Chem. Mater.* **2000**, *12* (8), 2363–2371.

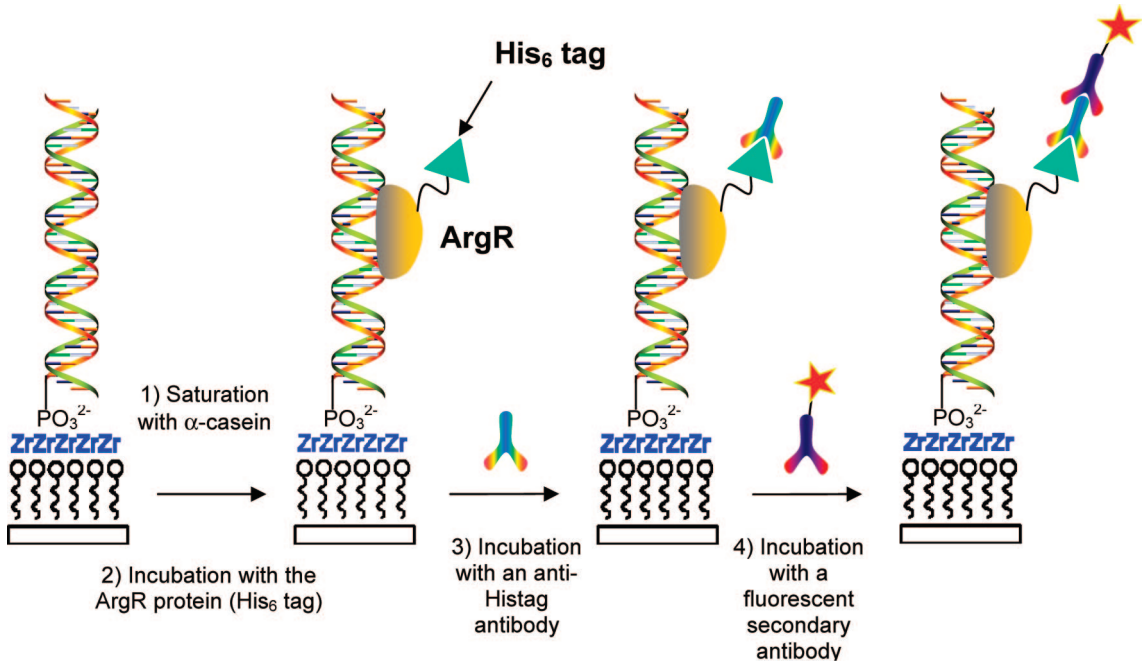

Figure 1. Schematic representation of the incubation process after spotting of the dsDNA probes.

by Langmuir–Blodgett deposition of an organophosphonic acid.[30–35] We have long utilized LB methods to prepare the zirconium phosphonate monolayers because the surface films formed in this way are of high quality, stable,[30,31,49] and highly reproducible, and the surface chemistry can be applied to any substrate material, permitting application of a wide range of surface analytical techniques on the same surface. Using the LB technique, octadecylphosphonic acid (ODPA) is spread at the air–water interface, compressed into a monolayer, and then transferred onto a substrate that is first made hydrophobic. The ODPA-coated substrate is then exposed to a solution of Zr^{4+} ions that bind to give a monolayer of the zirconated octadecylphosphonic acid (ODPA-Zr), which is exceptionally smooth and uniform.[50] The extremely strong binding of the zirconium ions cross-links the original monolayer and provides a stable, well-defined interface of zirconium phosphonate sites. The zirconium ions on the surface are active and react readily when exposed to phosphonate or phosphate groups, binding them to the surface.

In earlier work, we showed that oligonucleotides can be immobilized on the zirconium phosphonate surfaces and that phosphate terminated oligonucleotides are selectively adsorbed over those without terminal phosphates (see Supporting Information). [36] The terminal phosphate binds, but the phosphodiester groups of the backbone are not sufficiently basic to displace the hydroxide or oxide groups from the Zr^{4+} sites at the surface to form similar covalent linkages. Nonphosphorylated probes can physisorb to the surface but wash off with sufficiently stringent rinsing conditions, such as those used in subsequent passivation and hybridization steps.[51]

A ds-DNA/repressor interaction model is used to investigate the zirconium phosphonate surface for immobilizing dsDNA for use in microarrays and analyzing dsDNA/proteins interactions. After the dsDNA probes are spotted onto the ODPA-Zr modified glass slide, the typical experimental procedure can be broken into four steps (Figure 1).

First, a saturation of the surface is performed using a small protein to passivate unspotted areas of the array. The slides are then incubated with a hexahistidine-tagged protein repressor from *Thermotoga neapolitana* (ArgR), which interacts strongly ($K_d = 3 \times 10^{-9}$ M) with the *B. Stearothermopilus PargCo* promoter-operator from which the 19-mer dsDNA probe sequence (termed **X/compX**) was designed.[38] A second incubation is performed using a monoclonal antipolyhistidine antibody, and then a final incubation is performed using a fluorescent secondary antibody (Alexafluor 642). The best signal-to-noise ratios are observed when α-casein is used for the saturation step. This treatment inhibits nonspecific adsorption of the target protein and fluorescent secondary antibody but does not displace the covalently attached probes. Here, α-casein was found to be superior to the commonly used BSA (bovine serum albumin), presumably because it is rich in phosphate groups which favor higher binding to the zirconated surface.[52] The α-form was preferred to the β-form because it exhibited higher binding to the zirconated surface, likely because of its higher level of phosphorylation.[53]

Including a Spacer between the Probe and the Surface. For oligonucleotide microarrays, enhanced hybridization is expected

(45) Putvinski, T. M.; Schilling, M. L.; Katz, H. E.; Chidsey, C. E. D.; Mujsce, A. M.; Emerson, A. B. *Langmuir* **1990**, *6* (10), 1567–1571.
(46) Snover, J. L.; Byrd, H.; Suponeva, E. P.; Vicenzi, E.; Thompson, M. E. *Chem. Mater.* **1996**, *8* (7), 1490–1499.
(47) Thompson, M. E. *Chem. Mater.* **1994**, *6* (8), 1168–1175.
(48) Byrd, H.; Suponeva, E. P.; Bocarsly, A. B.; Thompson, M. E. *Nature* **1996**, *380* (6575), 610–612.
(49) Petruska, M. A.; Talham, D. R. *Langmuir* **2000**, *16* (11), 5123–5129.
(50) Bujoli, B.; Lane, S. M.; Nonglaton, G.; Pipelier, M.; Leger, J.; Talham, D. R.; Tellier, C. *Chem.—Eur. J.* **2005**, *11* (7), 1981–1988.
(51) Lane, S. M.; Monot, J.; Petit, M.; Tellier, C.; Bujoli, B.; Talham, D. R. *Langmuir*, in press.
(52) Zhou, H. J.; Xu, S. Y.; Ye, M. L.; Feng, S.; Pan, C.; Jiang, X. G.; Li, X.; Han, G. H.; Fu, Y.; Zou, H. *J. Proteome Res.* **2006**, *5* (9), 2431–2437.
(53) Cuccurullo, M.; Schlosser, G.; Cacace, G.; Malorni, L.; Pocsfalvi, G. *J. Mass Spectrom.* **2007**, *42* (8), 1069–1078.

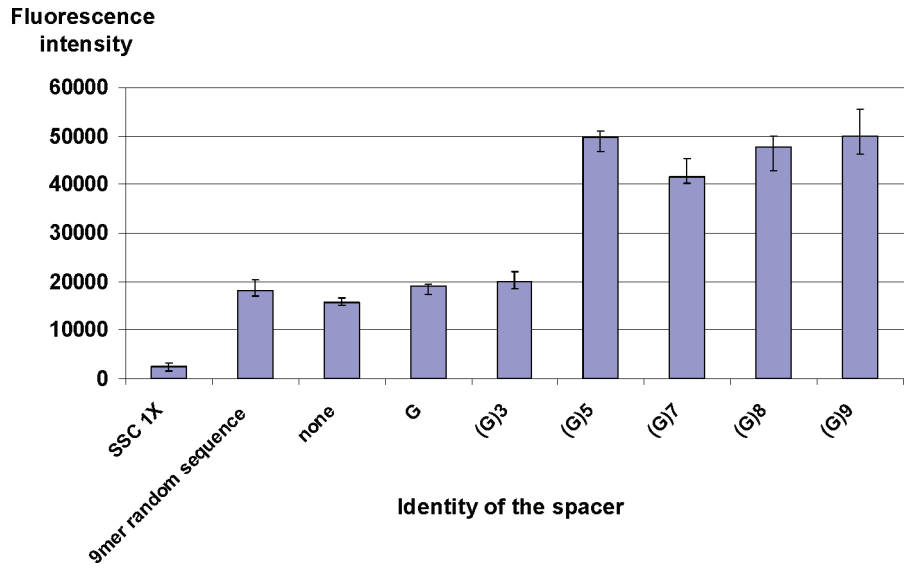

Figure 2. Fluorescence after incubation (as described in Figure 1) upon introduction of a polyG spacer to the probe. The slides were spotted with **5′P-(spacer)-X/5′P-(spacer)-compX** duplexes (10 μM). The data correspond to the median and interquartile range for three slides (18 spots per slide, for each probe). The slides were scanned at 85% of laser power and 80% of photomultiplier gain.

when the probe oligonucleotide is distanced from the support surface by a tether.[26,27,54–56] This observation, made for several other systems, is normally attributed to increasing the availability of the probe by distancing it from the surface and relieving steric crowding.[55] A tether may also reduce nonspecific binding of the probe to the surface. In this context, while exploring possible tethers for the attachment of single-stranded oligonucleotides on ODPA-Zr monolayers, we observed that short segments of guanine (G) oligomer lead to an increase in fluorescence after hybridization by a factor of 2 relative to cases in which no spacer is present. The poly-G spacer is more effective than other homonucleotide segments, and the most pronounced effect is observed for spacers [$(G)_n$] with $n = 7$–9. [36]

To investigate the effect of polyguanine spacers on the dsDNA/protein interaction, probes containing polyguanine spacers of different length ($n = 0$–9) were introduced between the terminal 5′-phosphate groups and the dsDNA probe sequence [termed **5′P-(spacer)-X/5′P-(spacer)-compX**] and the behavior was compared to that when a random 9-mer spacer is used. The results summarized in Figure 2 clearly show that the nature and the size of the spacer are critical.

The presence of $(G)_n$ spacers when $n \geq 5$ leads to an increase in fluorescence by a factor of 2.5 relative to the use of no spacer or a random 9-mer spacer. The "poly-G effect" observed for single-stranded DNA probes[36] used to detect DNA targets extends to double-strand DNA probes interacting with protein targets.

The reason for the influence of the guanine oligomer spacer is probably that, unlike other homopolymers, poly-G does not normally exist in a single-stranded form. G-rich sequences are able to form G-quadruplex structures, made up of G-quartet subunits with four coplanar guanines linked together by Hoogsteen hydrogen bonds. Within each quadruplex, the G-quartets stack and are stabilized by coordination of the carbonyl oxygen atoms in the guanines to specific monovalent cations, such as Na^+ or K^+.[57–64] Circular Dichroism (CD) has been used in the literature to examine the thermostability and the structures of G-quadruplexes present in telomeres.[65–72] It has been shown that the presence of G-quadruplex gave rise to characteristic CD bands: a positive band close to 260 nm for parallel G-quadruplex structures, while antiparallel structures led to a negative band at 260 nm and a positive one at 290 nm.[65] A standard protocol was thus used to probe the presence of such species in samples of the probe molecules,[73,74] and their CD spectra were compared when prepared in water versus 1X SSC

(54) Guo, Z.; Guilfoyle, R. A.; Thiel, A. J.; Wang, R. F.; Smith, L. M. *Nucleic Acids Res.* **1994**, *22* (24), 5456–5465.
(55) Shchepinov, M. S.; CaseGreen, S. C.; Southern, E. M. *Nucleic Acids Res.* **1997**, *25* (6), 1155–1161.
(56) Thiel, A. J.; Frutos, A. G.; Jordan, C. E.; Corn, R. M.; Smith, L. M. *Anal. Chem.* **1997**, *69* (24), 4948–4956.
(57) Aboulela, F.; Murchie, A. I. H.; Lilley, D. M. J. *Nature* **1992**, *360* (6401), 280–282.
(58) Aboulela, F.; Murchie, A. I. H.; Norman, D. G.; Lilley, D. M. J. *J. Mol. Biol.* **1994**, *243* (3), 458–471.
(59) Cheong, C. J.; Moore, P. B. *Biochemistry* **1992**, *31* (36), 8406–8414.
(60) Kang, C.; Zhang, X. H.; Ratliff, R.; Moyzis, R.; Rich, A. *Nature* **1992**, *356* (6365), 126–131.
(61) Laughlan, G.; Murchie, A. I. H.; Norman, D. G.; Moore, M. H.; Moody, P. C. E.; Lilley, D. M. J.; Luisi, B. *Science* **1994**, *265* (5171), 520–524.
(62) Phillips, K.; Dauter, Z.; Murchie, A. I. H.; Lilley, D. M. J.; Luisi, B. *J. Mol. Biol.* **1997**, *273* (1), 171–182.
(63) Smith, F. W.; Feigon, J. *Biochemistry* **1993**, *32* (33), 8682–8692.
(64) Davis, J. T. *Angew. Chem., Int. Ed.* **2004**, *43* (6), 668–698.
(65) Balagurumoorthy, P.; Brahmachari, S. K. *J. Biol. Chem.* **1994**, *269* (34), 21858–21869.
(66) Balagurumoorthy, P.; Brahmachari, S. K.; Mohanty, D.; Bansal, M.; Sasisekharan, V. *Nucleic Acids Res.* **1992**, *20* (15), 4061–4067.
(67) Dapic, V.; Abdomerovic, V.; Marrington, R.; Peberdy, J.; Rodger, A.; Trent, J. O.; Bates, P. J. *Nucleic Acids Res.* **2003**, *31* (8), 2097–2107.
(68) Giraldo, R.; Suzuki, M.; Chapman, L.; Rhodes, D. *Proc. Natl. Acad. Sci. U.S.A.* **1994**, *91* (16), 7658–7662.
(69) Hazel, P.; Huppert, J.; Balasubramanian, S.; Neidle, S. *J. Am. Chem. Soc.* **2004**, *126* (50), 16405–16415.
(70) Li, W.; Miyoshi, D.; Nakano, S.; Sugimoto, N. *Biochemistry* **2003**, *42* (40), 11736–11744.
(71) Li, W.; Wu, P.; Ohmichi, T.; Sugimoto, N. *FEBS Lett.* **2002**, *526* (1–3), 77–81.
(72) Rujan, I. N.; Meleney, J. C.; Bolton, P. H. *Nucleic Acids Res.* **2005**, *33* (6), 2022–2031.
(73) Paramasivan, S.; Rujan, I. N.; Bolton, P. H. *Methods* **2007**, *43*, 324–331.
(74) Read, M. A.; Neidle, S. *Biochemistry* **2000**, *39* (44), 13422–13432.

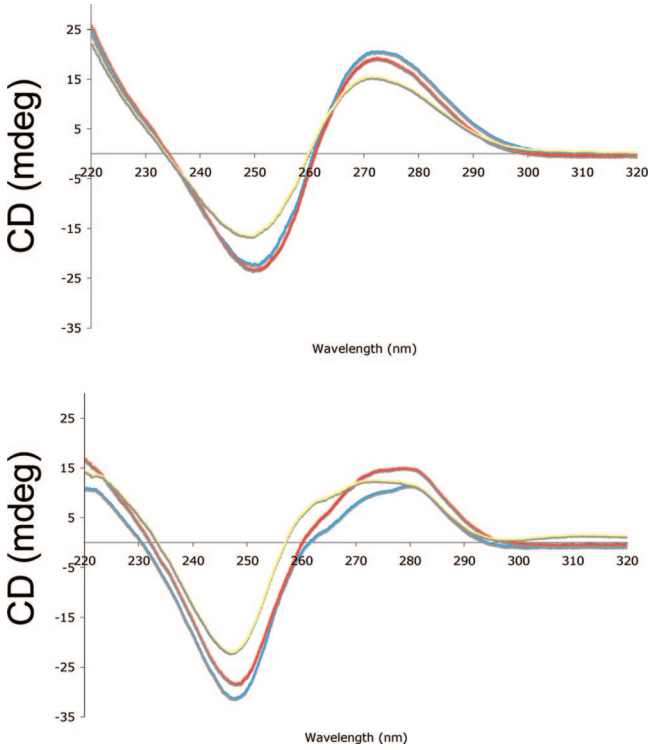

Figure 3. Compared CD spectra of **5′P-(spacer)-X/5′P-(spacer)-compX** [spacer = random 9-mer segment (blue), $(G)_1$ (red), or $(G)_9$ (yellow)] prepared in water (top) or 1X SSC [pH 6] (bottom). The probe with the G_9 spacer shows a positive band at 260 nm in SSC, indicating the presence of parallel G-quadruplex.

(Figure 3). A significant change of the CD spectrum of the **5′P-(G_9)-X/5′P-(G_9)-compX** samples, with the appearance of a positive band at 260 nm, indicates the formation of parallel G-quadruplexes in 1X SSC solution.

A possible consequence of the tendency of polyG segments to associate is the formation of multidentate aggregates that raise the avidity for the surface relative to individual probe duplexes. Support for this hypothesis comes from a detailed investigation of the polyG effect for single strand DNA probes which showed that the probes with the polyG spacer bound stronger and with twice the surface density relative to oligonucleotides with the same sequence and a polyA spacer.[51]

Effect of the Location of the Terminal Phosphate Groups on the Probe. With dsDNA probes, there are different possibilities for the placement of the surface anchoring group. Furthermore, with two chains, anchoring groups on each chain become a possibility leading one to question if the number and location of the phosphate groups have an effect on the binding ability and orientation of the dsDNA, which might affect subsequent interactions with the target protein. To the best of our knowledge, the use of two surface binding terminations for immobilizing dsDNA has not been previously reported. To investigate this issue, the "**X/compX**−ArgR" system was again used.

Several combinations of the terminal phosphate position on dsDNA probes were evaluated, as outlined in Figure 4. These arrangements include phosphate in the 5′ position of only one of the two strands (termed **5′P-$(G)_9$-X/compX**), phosphate groups in each of the 5′ positions (**5′P-$(G)_9$-X/5′P-$(G)_9$-compX**), phosphates in both of the 3′ positions (**X-$(G)_9$-P3′/compX-$(G)_9$-P3′**), phosphate groups in the 5′ and 3′ positions of one of the two strands (**5′P-$(G)_9$-X-$(G)_9$-P3′/compX**), and phosphate groups in the 5′ position for one of the two strands and in the 3′ position for the complementary strand (**5′P-$(G)_9$-X/compX-$(G)_9$-P3′**).

In all cases, a 9-mer guanine spacer was introduced between the terminal phosphate groups and the dsDNA probe sequence. As a control, a doubly phosphorylated duplex having no interaction domain with the ArgR protein (**5′P-$(G)_9$-Y/5′P-$(G)_9$-compY**) was also spotted under similar conditions.

The protein capture data are shown in Figure 5 and clearly demonstrate that the number and location of the phosphate groups are important. An increase in fluorescence by up to a factor of 2.4 is observed when two binding termini are present instead of one. The exception is for the case where the two phosphate groups are located on the same end of the dsDNA sequence. The highest fluorescence signal was measured when two phosphate groups are attached on the same strand within the duplex, while the nonspecific probe gave rise to a low signal, as expected.

Characterization of the dsDNA Probe Binding onto the ODPA-Zr Surface. The two most likely reasons for the variation in protein capture are that the phosphate linker and poly-G spacer arrangements lead to either differences in the number of probes that adsorb in a spot or an altered orientation of the probes and therefore different accessibility to the ArgR target. To better understand the factors responsible for the observed differences, careful surface characterization was undertaken to quantify the dsDNA probe binding onto the ODPA-Zr surface as a function of the location of the terminal phosphate groups.

First, in order to know if the fluorescence intensities were directly related to the binding efficiency of the probes, the optical thickness of the spots, after a mock saturation and before incubation with the protein, was measured for the six different probes using a novel optical technique called Sarfus, developed by Nanolane. The technology is based on an optical microscope working in a reflected differential interference contrast mode together with nonreflecting substrates termed "surfs" that increase the sensitivity of a traditional microscope up to 2 orders of magnitude.[75] This technique allows the direct visualization of nanoscale structures with a vertical resolution of less than 1 nm. At the same time, Sarfus allows rapid recording of wide field images, such as an entire micropattern made of hundreds of spots (more detail is provided in the Supporting Information).

As the top layer of the surf is made of silicon, the ODPA-Zr layer was deposited on its oxide surface under conditions similar to those used for glass slides. The geometrical thickness measured for the ODPA-Zr monolayer using the Sarfus technique is 1.9 nm in agreement with previous AFM measurements. Spots of the two different probes bearing the same linker and spacer groups, but differing in the dsDNA sequence (**5′P-$(G)_9$-X/5′P-$(G)_9$-compX** and **5′P-$(G)_9$-Y/5′P-$(G)_9$-compY**), were compared and shown to give comparable optical thickness (Figure 6), indicating that the amount of material bound is similar for the two probes. This control experiment confirms that the higher fluorescence observed for the former is due to the presence of the 19 base-pair domain recognized by the ArgR protein.

When the placement of the linkers is varied for the **X/compX** specific sequence, two main observations can be made. First, the variation of the optical thickness of the probe spots generally follows that of the fluorescence values for the different probes after protein capture. For example, the probes that yielded the

(75) Ausserre, D.; Valignat, M. P. *Nano Lett.* **2006**, *6* (7), 1384–1388.

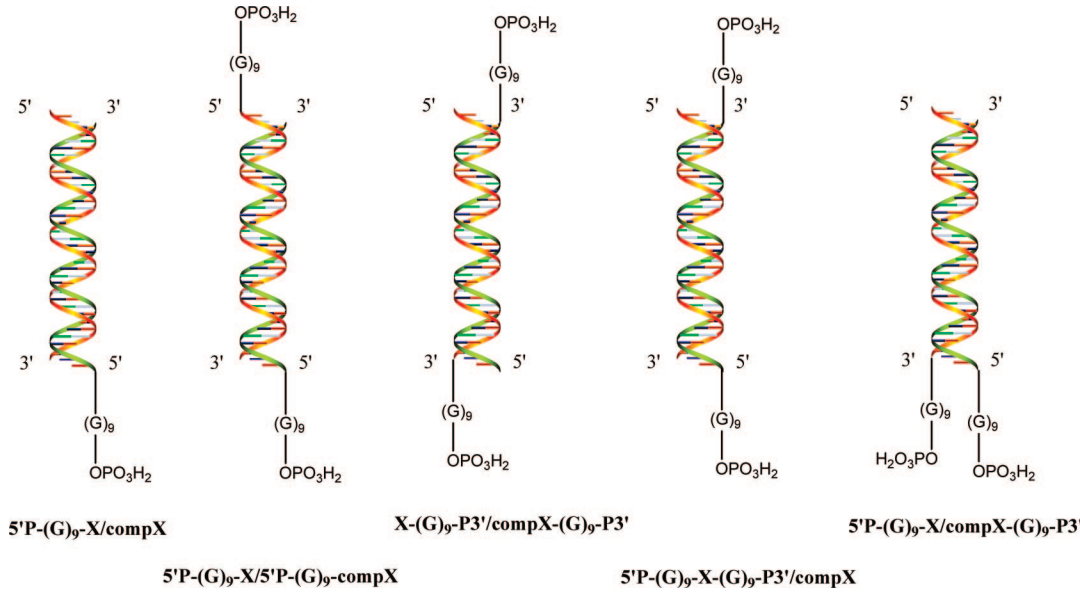

Figure 4. Schematic representation of the different combinations of terminal phosphate position for the dsDNA probes used in this study.

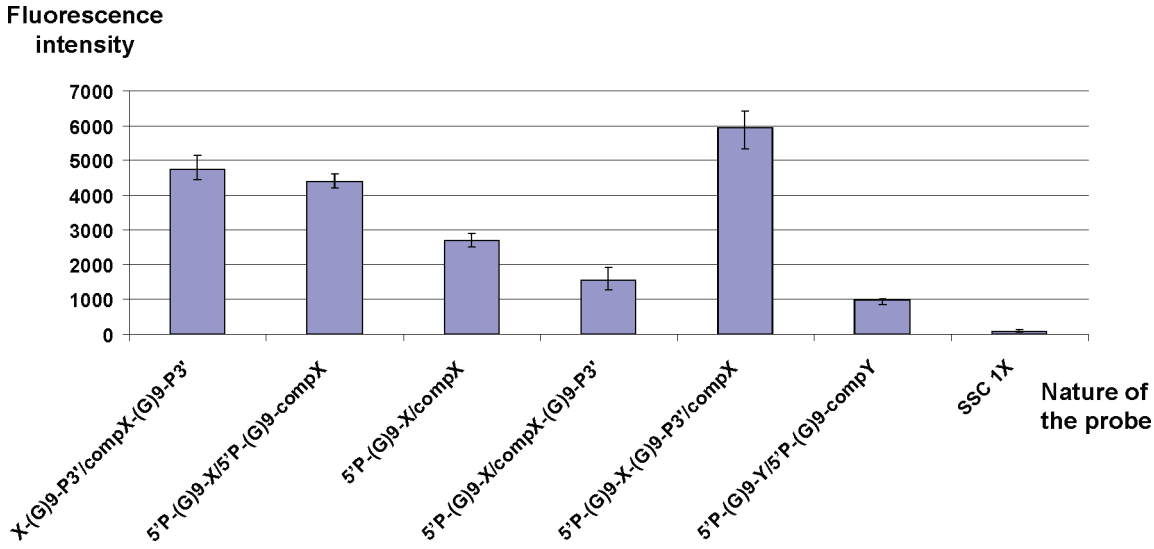

Figure 5. Fluorescence intensity upon incubation (as described in Figure 1) as a function of the number and location of terminal phosphate groups on the probe. The double-stranded **Y/compY** probe has no interaction domain with the ArgR protein. The data correspond to the median and interquartile range for 18 replicates per spotted probe (10 μM).

smallest ArgR protein capture, the singly phosphorylated double-stranded probe and the probe doubly phosphorylated at the same end, **5′P-(G)$_9$-X/compX-(G)$_9$-P3′**, have about one-half the optical thickness of the others, indicating that probe coverage is the primary reason for lower fluorescence detection in those cases. The second observation is that the optical thickness of all the probe spots range between 0.25 and 0.6 nm, which is small relative to the size of a dsDNA strand with a nominal mean width of ~2 nm and mean extended length of ~12.6 nm for a 37-mer,[76] thus suggesting that the dsDNA are lying flat on the surface with relatively low surface coverage.

Comparison of the Probes with Two Phosphate Linkers. The three probes with terminal phosphates on either end of the double strand that lead to the highest ArgR protein capture were investigated in more detail to better understand differences between them. Again, the presence of parallel G-quadruplexes in the spotting solutions was confirmed by CD measurements [see Supporting Information]. Previous work demonstrated that X-ray photoelectron spectroscopy can be used to quantify the surface coverage of phosphorylated oligonucleotides immobilized on zirconium-phosphonate surfaces.[77] With the help of an appropriate overlayer model, the DNA coverage (k) can be determined by relating the intensity of the N 1s signal originating from the oligonucleotide to the intensity of the Zr 3d peak from the zirconium phosphonate layer, the surface coverage of which is known. The surface coverages of the doubly phosphorylated probes, determined from XPS, are listed in Table 1. The XPS

(76) Kelley, S. O.; Barton, J. K.; Jackson, N. M.; McPherson, L. D.; Potter, A. B.; Spain, E. M.; Allen, M. J.; Hill, M. G. *Langmuir* **1998**, *14* (24), 6781–6784.

(77) Lane, S. M.; Monot, J.; Petit, M.; Bujoli, B.; Talham, D. R. *Colloids Surf., B* **2007**, *58* (1), 34–38.

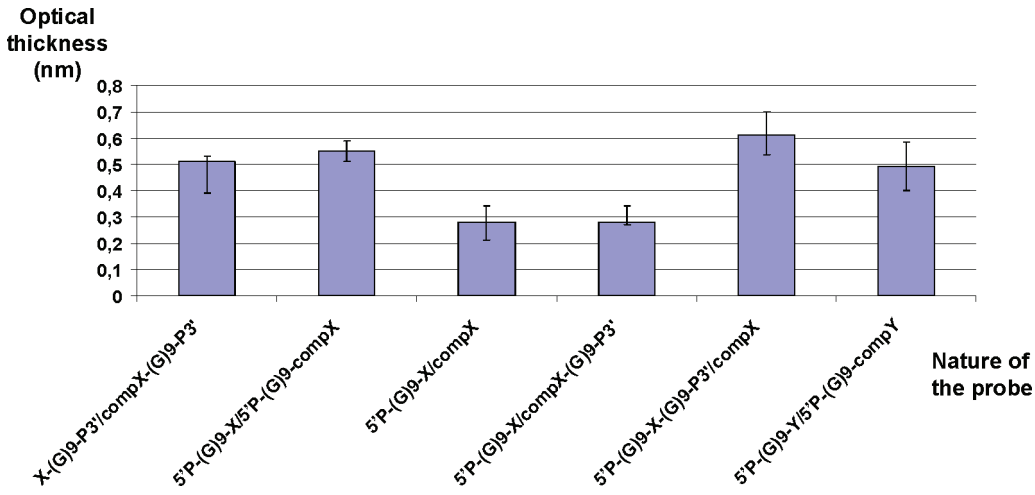

Figure 6. Optical thickness of the spots measured by the Sarfus technique before saturation and incubation with ArgR protein, as a function of the number and location of terminal phosphate groups on the probe. The double-stranded **Y/compY** probe has no interaction domain with the ArgR protein. The data correspond to the median and interquartile range for 18 replicates per spotted probe (10 μM). The ODPA-Zr film was deposited on a Nanolane surf.

Table 1. XPS Analysis of the dsDNA Surface Coverage, Sarfus Optical Thickness and AFM Thickness for Spotted Probes before Incubation with ArgR Protein, and Fluorescence Intensity Recorded after Incubation

	characterization of the spots				
spotted probe	*k* XPS ds-DNA coverage (molecules/cm^2 $\times$ 10^{-11})[a]	Fluorescence intensity (arbitrary units)	*l*, Sarfus optical thickness (nm)	*m*, AFM thickness (nm)	*l*/*mk* ($\times$ 10^{12})
5′P-(G)$_9$-X/5′P-(G)$_9$-compX	4.0(5)	4400	0.55	0.61	2.2
X-(G)$_9$-P3′/compX-(G)$_9$-P3′	5.6(8)	4700	0.51	0.46	2.0
5′P-(G)$_9$-X-(G)$_9$-P3′/compX	2.6(1)	5900	0.61	1.01	2.3

[a] Average of at least four experiments.

results are consistent with the low surface coverage suggested by the Sarfus data of Figure 6. The measured surface coverage, (2.6–5.6) $\times$ 10^{-11} molecules/cm^2, is significantly less than $\sim 10^{13}$ molecules/cm^2 in a close packed monolayer of DNA probes standing on end. At this level of surface coverage the probes lay on the surface, accounting for the small spot height observed by Sarfus.

Another observation from the XPS data is that the lowest surface coverage is for the probe with both phosphate groups on the same strand, **5′P-(G)$_9$-X-(G)$_9$-P3′/compX**, approximately one-half that of the **X-(G)$_9$-P3′/compX-(G)$_9$-P3′** probe, although the former yields the highest target capture based on fluorescence detection. The difference in target capture efficiency may be related to how the probes are presented on the surface. Evidence for differences in the organization of the probes comes from correlating the surface coverage measurements with thickness measurements. The Sarfus apparatus can be combined with AFM in such a way that areas of interest can be measured using the Sarfus microscope and then shifted on a mobile stage to allow the same area of the sample to be imaged by AFM, making it possible to measure for one spot, both the geometrical thickness (*m*) and optical thickness (*l*). An example is shown in Figure 7, and data for the three doubly phosphorylated probes are collected in Table 1.

The optical thickness is related to the geometrical thickness modified by the refractive index of the dsDNA layer, with an expected linear relationship between the latter and the probe surface coverage, *k*, since the three probes have identical chemical formulas.[78,79] Using the data obtained from the XPS and AFM-SARFUS experiments, the quantity *l*/*mk* should be constant in a consistent set of experiments, as shown in Table 1.

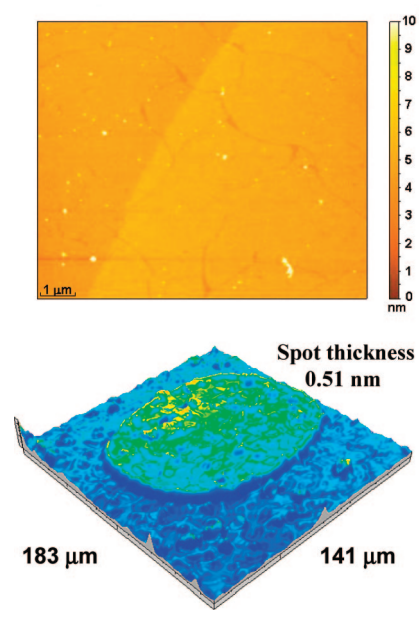

Figure 7. AFM (top) and Sarfus (bottom) images of the same **5′P-(G)$_9$-X/5′P-(G)$_9$-compX** spot before saturation and incubation with ArgR protein, using a Sarfus/AFM combined device. The ODPA-Zr film was deposited on a Nanolane surf.

(78) Kitamura, N.; Fukumi, K.; Nishii, J.; Ohno, N. *J. Appl. Phys.* **2007**, *101* (12), 123533.

(79) Wang, P.; Beck, A.; Korner, W.; Scheller, H.; Fricke, J. *J. Phys. D: Appl. Phys.* **1994**, *27* (2), 414–418.

Upon comparing the three probes, the trend in geometrical thickness is opposite the order of the measured surface coverage. Although the surface coverage for the **5′P-(G)$_9$-X-(G)$_9$-P3′/compX** probe is one-half that of **X-(G)$_9$-P3′/compX-(G)$_9$-P3′**, the AFM-determined thickness is significantly higher (1.01 versus 0.46 nm), thereby indicating that the **5′P-(G)$_9$-X-(G)$_9$-P3′/compX** probes are oriented differently, more extended away from the support. Remembering that the thickness is small and that the probe mostly lays flat on the surface, this increase in height is likely bending of the DNA strand between the two anchor points. This orientation difference apparently facilitates the dsDNA/ArgR interaction, accounting for the higher protein capture efficiency with the **5′P-(G)$_9$-X-(G)$_9$-P3′/compX** probe.[80,81] The data suggest a third orientation for the probe with two phosphate groups at the primary 5′, 5′ positions. The surface coverage falls between the other two, yet results in similar target fluorescence intensities suggesting this orientation gives intermediate protein capture efficiency.

Conclusion

Phosphorylated double-stranded DNA probes bind strongly to glass substrates coated with a zirconium phosphonate monolayer. A dsDNA/protein interaction model was used to investigate the efficacy of binding of the probes and their subsequent ability to capture the protein target. The sensitivity and specificity of the arrays are enhanced when polyguanine spacers are present, and the best results were observed when two phosphate groups are introduced on the two ends (3′ and 5′) of one of the two strands of the DNA duplex. As far as we are aware, this is the first time that two functional groups have been introduced on dsDNA for their immobilization as microarrays. The effect of their location on the probes has been shown to influence probe molecule surface binding and orientation, along with protein capture efficiency. This analysis was made possible through the original use of a combination of surface characterization techniques, including XPS, Sarfus, and AFM, which allowed collecting information regarding relevant features for the different probes when bound to the surface. Finally, additional interest of the zirconium phoshonate substrate methodology lies in the fact that terminal phosphorylation of oligonucleotides can be easily achieved using enzymatic (T4 polynucleotide kinase) routes, opening the way to the potential use of PCR products as probes.

Acknowledgment. This work was partially supported by the CNRS (Programme “Puces à ADN” and Action CNRS - Etats-Unis 2005 n° 3310), the Institut National de la Santé et de la Recherche Médicale, the “Association Française contre les Myopathies” and the “Région Pays de la Loire”. I.G. was supported by a grant from Genopôle Ouest. Support from the U.S. National Science Foundation through Grants INT-9981579 and CHE-0514437 (D.R.T.) is also acknowledged. The authors thank NANOLANE and SCIENTEC for their contributions in the experiments and useful discussions. The authors thank Dr. Marie-Claire ARNAUD for help in the biological experiment and useful advices, and V. Sakanyan for providing the ArgR gene.

Supporting Information Available: Complete reference listings for refs 3 and 11, description of the Sarfus technology, figure showing the concept for immobilizing phosphate terminated oligonucleotides on zirconated organophosphonate treated slides through coordinate covalent linkages, Sarfus image of a spotted area, photograph of the Sarfus-AFM combined device, CD comparison of **5′P-(G)$_9$-X-(G)$_9$-P3′/compX** prepared in water and 1X SSC [pH 6], CD comparison of **5′P-(G)$_9$-X/5′P-(G)$_9$-compX** prepared in water and 1X SSC [pH 6], CD comparison of **5′P-(G)$_1$-X/5′P-(G)$_1$-compX** prepared in water and 1X SSC [pH 6], CD comparison of **5′P-(9 mer random)-X/5′P-(9 mer random)-compX** prepared in water and 1X SSC [pH 6]. This material is available free of charge via the Internet at http://pubs.acs.org.

JA711427Q

(80) Ni, J. P.; Sakanyan, V.; Charlier, D.; Glansdorff, N.; Van Duyne, G. D. *Nat. Struct. Biol.* **1999**, *6* (5), 427–432.
(81) Tian, G. L.; Lim, D. B.; Carey, J.; Maas, W. K. *J. Mol. Biol.* **1992**, *226* (2), 387–397.